

Crosstalk Prediction of Handmade Cable Bundles for New Energy Vehicles

Jinghua Guo^{1,*} and Yuanyuan Liu^{1,2}

¹School of Intelligent Manufacturing
Wuxi Vocational College of Science and Technology, Wuxi, Jiangsu, 214028, China
*2697244379@qq.com

²School of IoT Engineering
Jiangnan University, Wuxi, Jiangsu, 214122, China

Abstract – This paper presents an effective solution for the crosstalk prediction of handmade cable bundles. The outer- and inner-layer topology of the cross section are analyzed respectively, combined with the actual physical model of the cable bundles. The cascading method is used to deal with the relationship between the structure of cable bundles and the distributed per unit length (p.u.l.) parameter matrices. The random exchange of the wires in the cable bundles is equivalent to the row–column transformation of the p.u.l. parameter matrix, and the values of the p.u.l. parameter matrix after the transformation are modified by equal interval rotation degree. Then, the unconditionally stable finite difference time domain (FDTD) method is used to solve the crosstalk. The verification analysis shows that the change of the element value of the p.u.l. parameter matrix caused by the rotation of the cross-section relative to the ground cannot be ignored. The accuracy of the proposed method is evaluated through comparison to the probability method for a seven-core handmade cable bundles, especially in the high frequency.

Index Terms – Handmade cable bundles, crosstalk, multiconductor transmission line, electromagnetic interference, finite-difference time-domain (FDTD).

I. INTRODUCTION

Electromagnetic compatibility (EMC) plays an important role in the field of automotive electronics [1]. New energy vehicles have been rapidly developed and applied. Compared with traditional vehicles, new energy vehicles need more electronic devices with high voltage, high current, and high frequency. Multiconductor transmission line (MTL) is a bridge to realize energy and signal transmission among electronic devices. Therefore, the electromagnetic environment of new energy vehicles is more complex.

Generally, some transmission lines with similar characteristics will be tightly tied together by hand for

the sake of simplicity and beauty. In addition, the assembly of the automobile wiring harness is completed manually from offline, crimping, subassembly, assembly, inspection, and packaging. Therefore, the relative position among the wires in the handmade cable bundles is random. The handmade cable bundles are a kind of random wiring harnesses. A large number of wires are closely arranged, and unintentional electromagnetic radiation may cause crosstalk [2].

Changes in the position between the wires will cause changes in system parameters [3]. It is very important to accurately predict this effect in the early stage of design. The discretization method is introduced by P. Besnier to establish the nonuniform MTL model [4]. The nonuniform MTL is approximated as a large number of small uniform MTLs connected end to end. Monte Carlo (MC) method has been used to analyze the crosstalk of random exchange of wires [5]. The random wiring harness is modeled by random midpoint displacement (RMD) algorithm [6], but the reduced model is too rough. The random displacement spline interpolation (RDSI) method is proposed in [7] considering the smooth change between cascaded segments on the basis of RMD. However, RDSI has a high requirement for the numerical solution of wiring harness and the amount of calculation is large. Assuming that the topological shape of the harness cross section relative to the ground is constant, only the exchange of the position of the wires exists in wiring harness, and the “reasonable worst-case” crosstalk of the wiring harness is predicted by using the probability distribution of the per unit length (p.u.l.) parameter matrix of a single cross section [8][9]. Considering that there is only the exchange of adjacent wires in the harness, the random bundles of twisted wire pairs are modeled and the response value is solved by using the commercial software FEKO based on the method of moments [10]. A simple mathematical model of handmade cable bundles is proposed in [11], which is based on the cascading method and MC method. In all aforementioned papers,

the influence of the rotation of the topological shape of the harness cross section relative to the ground on the crosstalk has not been considered, and the influence is discussed in detail in this paper.

The finite-difference time-domain (FDTD) method is a common method in the field of crosstalk solution. The FDTD method can segment time and space, and can effectively describe the nonuniformity along with the cable bundles. The conventional FDTD method needs to meet the stability conditions to iterative convergence, which seriously affects the efficiency of the solution [15–17]. Therefore, combined with the unconditionally stable difference scheme [18], the crosstalk solution method of handmade cable bundles is derived in this paper.

The rest of this paper is arranged as follows. The model of handmade cable bundles is established in Section II. In Section III, the distribution p.u.l. parameter matrix of the model is solved. Section IV gives the experimental verification and analysis. Finally, Section V draws the conclusion.

II. MODELING OF HANDMADE CABLE BUNDLES

The application of handmade cable bundles under a certain type of car window is shown in Figure 1. The wire harness has the characteristics that the wires are close to each other, and the relative positions between the wires change randomly. Several wire types are shown in Figure 1. However, the physical parameters of the wires, including the material and radius of the conductor, the material and thickness of the insulation, are assumed to be consistent due to the simplification of the model. All the wires are close together to keep the topological shape of the outer circle of the cross section unchanged.

The cross section equivalent model is shown in Figure 2. The blue- and red-dashed lines represent the outer layer topology and the inner layer topology respectively. The cross section of different points along the cable bundles can be realized in two steps. The wires position from cross section 1 to cross section 2 are first exchanged. The second is the rotation of the inner topology from cross section 2 to cross section 3.

Handmade cable bundles are segmented by using cascade method and differential method. Cable bundles in each segment are regarded as parallel MTLs, and the position of wires in each cross section is independent of each other. Cable bundles with different twisting degrees can be equivalent to N -segment cascaded transmission line, which can be obtained from the empirical formula:

$$N = \begin{cases} \lceil \beta l_{cable} \rceil, & \beta > 1/l_{cable} \\ 1, & \beta \leq 1/l_{cable} \end{cases}, \quad (1)$$

where, β indicates the twisting degree (segment/m), obtained from experience. The physical meaning of twisting degree is the degree of random exchange



Fig. 1. Handmade cable bundles under car window.

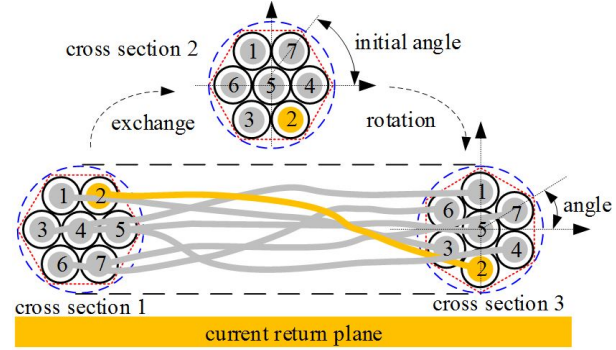


Fig. 2. Cross section equivalent model of handmade cable bundles.

between wires in the same length of the cable bundles, corresponding to the number of cascaded segments. l_{cable} stands for the length of the cable bundles (m), and $\lceil \cdot \rceil$ is the round down symbol.

III. PARAMETER MATRIX AND CROSSTALK SOLUTION OF HANDMADE CABLE BUNDLES

A. MTL model

The p.u.l. equivalent circuit of n -core MTLs on the current return plane is shown in Figure 3. The current return plane is selected as the reference conductor. dz stands for the infinitely short transmission line. l , c , g , and r are the p.u.l. parameters. r_i and r_j are the resistance. l_{ii} and l_{ij} are the self-inductance and mutual inductance, respectively. c_{ii} and c_{ij} are the self-capacitance and mutual capacitance, respectively. g_{ii} and g_{ij} are the self-conductivity and mutual conductivity, respectively. The matrix form is

$$\mathbf{X} = \begin{bmatrix} x_{11} & x_{12} & \cdots & x_{1i} & \cdots & x_{1j} & \cdots & x_{1n} \\ x_{21} & x_{22} & \cdots & x_{2i} & \cdots & x_{2j} & \cdots & x_{2n} \\ \vdots & \vdots & \ddots & \vdots & \vdots & \vdots & \vdots & \vdots \\ x_{i1} & x_{i2} & \cdots & x_{ii} & \cdots & x_{ij} & \cdots & x_{in} \\ \vdots & \vdots & \vdots & \vdots & \ddots & \vdots & \vdots & \vdots \\ x_{j1} & x_{j2} & \cdots & x_{ji} & \cdots & x_{jj} & \cdots & x_{jn} \\ \vdots & \vdots & \vdots & \vdots & \vdots & \vdots & \ddots & \vdots \\ x_{n1} & x_{n2} & \cdots & x_{ni} & \cdots & x_{nj} & \cdots & x_{nn} \end{bmatrix}, \quad (2)$$

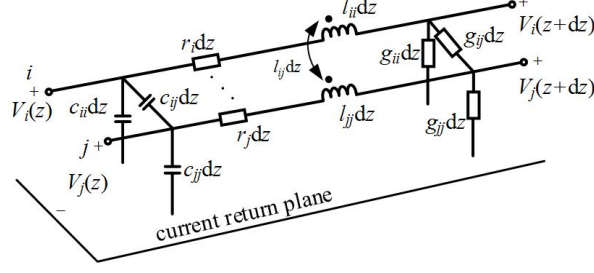


Fig. 3. The p.u.l. equivalent circuit of n -core MTL.

where X is p.u.l. the parameter matrix L , C , G , or R , x is the corresponding element of l , c , g , and r , $x_{ij} = x_{ji}$. X is a symmetric parameter matrix of order n , the upper and lower triangular elements of the matrix are equal, and the elements in the matrix can be divided into main diagonal and non-main diagonal elements. The main diagonal element value of the parameter matrix is mainly determined by the height of the wire from the reference plane since the physical parameters of the wire are consistent. Similar to the main diagonal elements, the non-main diagonal elements are determined by the relative position between wires and their height from the reference plane.

B. Parameter matrix analysis

The wire position exchange in the cross section can be equivalent to the arrangement and combination of wire numbers in the inner layer topology when changing from cross section 1 to cross section 2 in Figure 2.

The distance between the conductors and the distance between the conductor and the reference plane are constant if the topology of the inner layer is consistent. Therefore, the p.u.l. mutual inductance, self-inductance, mutual capacitance, and self-capacitance will remain unchanged. When only wire i and wire j are exchanged, the parameter matrix of the cable bundles is:

$$\mathbf{X}' = \begin{bmatrix} x_{11} & x_{12} & \cdots & x_{1j} & \cdots & x_{1i} & \cdots & x_{1n} \\ x_{21} & x_{22} & \cdots & x_{2j} & \cdots & x_{2i} & \cdots & x_{2n} \\ \vdots & \vdots & \ddots & \vdots & \vdots & \vdots & \vdots & \vdots \\ x_{j1} & x_{j2} & \cdots & x_{jj} & \cdots & x_{ji} & \cdots & x_{jn} \\ \vdots & \vdots & \vdots & \vdots & \ddots & \vdots & \vdots & \vdots \\ x_{i1} & x_{i2} & \cdots & x_{ij} & \cdots & x_{ii} & \cdots & x_{in} \\ \vdots & \vdots & \vdots & \vdots & \vdots & \vdots & \ddots & \vdots \\ x_{n1} & x_{n2} & \cdots & x_{nj} & \cdots & x_{ni} & \cdots & x_{nn} \end{bmatrix}. \quad (3)$$

The transformation of the parameter matrix in (3) and (2) can be expressed as:

$$\mathbf{X}' = \mathbf{P}\mathbf{X}\mathbf{P}, \quad (4)$$

where \mathbf{P} is the elementary matrix after exchanging rows i and j . When the inner layer topology is the same, the two kinds of cross sections can always be obtained by exchanging each other for up to $n-1$ times.

The inner layer topology has a certain degree of rotation difference with respect to the reference plane when changing from cross section 2 to cross section 3 in Figure 2, and the clockwise direction is taken as the rotation direction. The inner layer topology is consistent with the initial inner layer topology after rotating 60° clockwise in the seven-core cable bundles. Therefore, only rotation from 0° to 60° needs to be considered. The rotation of the inner layer topology affects the position of each wire to the ground.

The effect of \mathbf{R} and \mathbf{G} on crosstalk actually is small, which can be ignored. \mathbf{L} and \mathbf{C} play a decisive role in crosstalk. The cross section of handmade cable bundles under the mirror method is shown in Figure 4. The right side is the reference cross section of rotation degree. i' and j' are the mirror images of wire i and wire j respectively. According to Ampere's law, the self-inductance of wire i is:

$$l_i = \frac{\psi_i}{I_i} = \frac{\mu_0}{2\pi} \ln\left(\frac{h_i}{r_{wi}}\right) + \frac{\mu_0}{2\pi} \ln\left(\frac{2h_i}{h_i}\right) = \frac{\mu_0}{2\pi} \ln\left(\frac{2h_i}{r_{wi}}\right), \quad (5)$$

where μ_0 is the permeability in vacuum. ψ_i is the magnetic flux of wire i and reference plane when only wire i is excited. I_i is the current in wire i . r_{wi} is the conductor radius of the wire i . The self-inductance is only related to the height above the ground and its radius. The change of height before and after rotation is

$$\Delta h_i = \Delta h_j = 2(r_{wi} + r_{ti}) [\cos\theta_0 - \cos(\theta + \theta_0)], \quad (6)$$

where r_{ti} is the thickness of the insulating layer, and θ_0 is the angle shown in Figure 4.

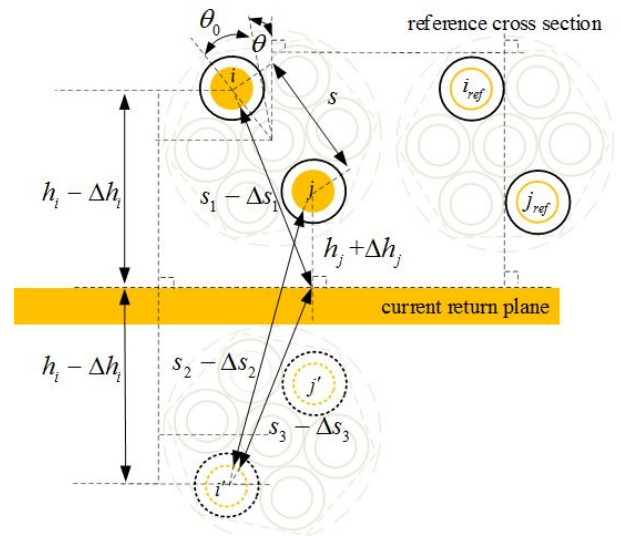


Fig. 4. Cross section of handmade cable bundles under the mirror image method.

The mutual inductance of wire i and wire j is:

$$l_{ij} = \frac{\psi_{ij}}{I_i} = \frac{\mu_0}{2\pi} \ln\left(\frac{s_1}{s}\right) + \frac{\mu_0}{2\pi} \ln\left(\frac{s_2}{s_3}\right) = \frac{\mu_0}{2\pi} \ln\left(\frac{s_2}{s}\right), \quad (7)$$

where s is the center distance between wire i and wire j . s_1 is the distance between the wire i and the projection point of the wire j on the reference ground. s_2 is the distance between the wire j and the wire i' . s_3 is the distance between the wire i' and the projection point of wire j on the reference ground. The mutual inductance is only related to s_2 and s . The change of s_2 before and after rotation is:

$$\Delta s_2 = \sqrt{(h_i + h_j)^2 + s \cdot \sin\theta_0} - \sqrt{(h_i + h_j)^2 + s \cdot \sin(\theta + \theta_0)}. \quad (8)$$

It can be seen from (5)–(8) that the element values of the inductance parameter matrix change with the change of rotation angle θ . The inductance parameters of the wire in the cable bundles with or without insulation layer can be calculated according to (5) and (7). The capacitance matrix without insulation is

$$\mathbf{C} = \mu_0 \varepsilon_0 \mathbf{L}^{-1}, \quad (9)$$

where ε_0 is the permittivity in vacuum.

The rotation of the cross section to the ground changes the parameter matrix of \mathbf{C} and \mathbf{L} when the conductor is uninsulated. The finite element method (FEM) is not limited by the insulation layer, but its solving process is complex. The parameter matrix of parallel MTL can be quickly extracted by commercial software ANSYS Q3D based on FEM.

The changes of Δh_i and Δs_2 caused by small rotation angle are also small. In the interval $[0, 60^\circ)$, a series of parameter matrices with equal interval are selected as the parameter matrix library of cable bundles to describe the rotation of cross section. The smaller the rotation degree interval is, the larger the parameter matrix library is, the more accurate the model is and the longer the consumption time is.

C. Crosstalk solution

The handmade cable bundles model described in this paper has the characteristics of cascade, and the FDTD method has the characteristics of spatial segmentation. Therefore, the FDTD method can be used to solve the handmade cable bundles. The conventional FDTD method needs to meet the stability condition to converge, while the difference scheme proposed by Kambiz Afrooz is unconditionally stable when applied to solve the transmission line equation [18]. In this section, the crosstalk solution of handmade cable bundles is mainly realized by combining with the difference scheme proposed by Kambiz Afrooz.

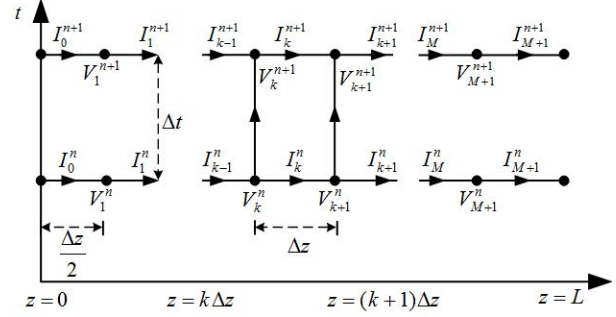


Fig. 5. Schematic diagram of voltage and current on MTL after discretization.

The telegraph equations of MTL are [19]:

$$\frac{\partial}{\partial z} \mathbf{V}(z, t) = -\mathbf{R}(z) \mathbf{I}(z, t) - \mathbf{L}(z) \frac{\partial}{\partial t} \mathbf{I}(z, t), \quad (10a)$$

$$\frac{\partial}{\partial z} \mathbf{I}(z, t) = -\mathbf{G}(z) \mathbf{V}(z, t) - \mathbf{C}(z) \frac{\partial}{\partial t} \mathbf{V}(z, t), \quad (10b)$$

where $\mathbf{V}(z, t)$ and $\mathbf{I}(z, t)$ are the voltage and current at time t at point z on the MTL respectively. The MTL is divided into M segments. The values of $\mathbf{R}(z)$, $\mathbf{L}(z)$, $\mathbf{G}(z)$, and $\mathbf{C}(z)$ at different positions on the handmade cable bundles are different. The parameter matrix of segment k is expressed as \mathbf{R}_k , \mathbf{L}_k , \mathbf{G}_k , and \mathbf{C}_k respectively.

The forward and backward difference approximations are made for the derivatives of z in (10a) and (10b) respectively:

$$\frac{V_{k+1} - V_k}{\Delta z} = -\mathbf{R}_k \mathbf{I}_k - \mathbf{L}_k \frac{\partial \mathbf{I}_k}{\partial t}, \quad (11)$$

$$\frac{I_k - I_{k-1}}{\Delta z} = -\mathbf{G}_k \mathbf{V}_k - \mathbf{C}_k \frac{\partial \mathbf{V}_k}{\partial t}, \quad (12)$$

where Δz is the spatial step, $\mathbf{V}_k = \mathbf{V}(k\Delta z, t)$, $\mathbf{I}_k = \mathbf{I}(k\Delta z, t)$. The form can be expressed as:

$$\mathbf{V}_{k+1} - \mathbf{V}_k + \Delta z \mathbf{R}_k \mathbf{I}_k + \Delta z \mathbf{L}_k \frac{\partial \mathbf{I}_k}{\partial t} = 0, \quad k = 1, \dots, M, \quad (13)$$

$$\mathbf{I}_k - \mathbf{I}_{k-1} + \Delta z \mathbf{G}_k \mathbf{V}_k + \Delta z \mathbf{C}_k \frac{\partial \mathbf{V}_k}{\partial t} = 0, \quad k = 2, \dots, M. \quad (14)$$

The MTL after discretization is shown in Figure 5, the subscript indicates the position of the MTL and the superscript represents the time, Δt is the time step. The terminal diagram of MTL is shown in Figure 6. \mathbf{R}_S and \mathbf{R}_L are the $n \times n$ dimensional impedance matrix of the source end and the load end of the MTL respectively, and \mathbf{V}_S is the n dimensional vector of excitation. Terminal conditions can be expressed as:

$$\mathbf{I}_0 = \frac{\mathbf{V}_S - \mathbf{V}_1}{\mathbf{R}_S} = \mathbf{I}_S - \frac{\mathbf{V}_1}{\mathbf{R}_S}, \quad (15)$$

$$\mathbf{I}_{M+1} = \frac{\mathbf{V}_{M+1}}{\mathbf{R}_L}, \quad (16)$$

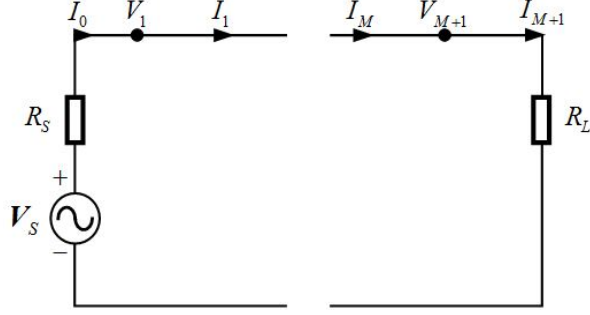


Fig. 6. Schematic diagram of terminal conditions of MTL after discretization.

where

$$I_S = \frac{V_S}{R_S}. \quad (17)$$

The Δz is replaced by $\Delta z/2$ for $k = 1$, and (15) is

$$I_1 - I_S + \left(\frac{\Delta z \mathbf{G}_1}{2} + \frac{1}{R_S} \right) \mathbf{V}_1 + \frac{\Delta z \mathbf{C}_1}{2} \frac{\partial \mathbf{V}_1}{\partial t} = 0. \quad (18)$$

The Δz is replaced by $\Delta z/2$ for $k = M+1$, and (16) is

$$I_M - \left(\frac{\Delta z \mathbf{G}_{M+1}}{2} + \frac{1}{R_L} \right) \mathbf{V}_{M+1} - \frac{\Delta z \mathbf{C}_{M+1}}{2} \frac{\partial \mathbf{V}_{M+1}}{\partial t} = 0. \quad (19)$$

The iterative equations are composed of (13), (14), (18), and (19), which are expressed in the form of matrix:

$$\begin{aligned} \mathbf{V}^{n+1} &= \left(\left(\frac{\tilde{\mathbf{G}}}{2} + \frac{\tilde{\mathbf{C}}}{\Delta t} \right) - \frac{\mathbf{A}}{4} \left(\frac{\tilde{\mathbf{R}}}{2} + \frac{\tilde{\mathbf{L}}}{\Delta t} \right)^{-1} \mathbf{B} \right)^{-1} \\ &\cdot \left\{ \frac{\mathbf{I}_S^n + \mathbf{I}_S^{n+1}}{2} - \left(\left(\frac{\tilde{\mathbf{G}}}{2} - \frac{\tilde{\mathbf{C}}}{\Delta t} \right) - \frac{\mathbf{A}}{4} \left(\frac{\tilde{\mathbf{R}}}{2} + \frac{\tilde{\mathbf{L}}}{\Delta t} \right)^{-1} \mathbf{B} \right) \mathbf{V}^n \right. \\ &\quad \left. - \left(\frac{\mathbf{A}}{2} - \frac{\mathbf{A}}{2} \left(\frac{\tilde{\mathbf{R}}}{2} + \frac{\tilde{\mathbf{L}}}{\Delta t} \right)^{-1} \left(\frac{\tilde{\mathbf{R}}}{2} - \frac{\tilde{\mathbf{L}}}{\Delta t} \right) \right) \mathbf{I}^n \right\}, \quad (20) \\ \mathbf{I}^{n+1} &= \left(\frac{\mathbf{R}}{2} + \frac{\mathbf{L}}{\Delta t} \right)^{-1} \\ &\times \left\{ \left(\frac{\mathbf{L}}{\Delta t} - \frac{\mathbf{R}}{2} \right) \mathbf{I}^n - \frac{\mathbf{B}}{2} (\mathbf{V}^n + \mathbf{V}^{n+1}) \right\}, \quad (21) \end{aligned}$$

where the superscript T denotes transpose,

$$\mathbf{A} = \begin{bmatrix} \mathbf{I} & 0 & 0 & \cdots & 0 & 0 \\ -\mathbf{I} & \mathbf{I} & 0 & \cdots & 0 & 0 \\ 0 & -\mathbf{I} & \mathbf{I} & \cdots & 0 & 0 \\ \vdots & \vdots & \vdots & \vdots & \vdots & \vdots \\ 0 & 0 & 0 & \cdots & -\mathbf{I} & \mathbf{I} \\ 0 & 0 & 0 & \cdots & 0 & -\mathbf{I} \end{bmatrix}, \quad (22)$$

$$\mathbf{B} = \begin{bmatrix} -\mathbf{I} & \mathbf{I} & 0 & \cdots & 0 & 0 \\ 0 & -\mathbf{I} & \mathbf{I} & \cdots & 0 & 0 \\ \vdots & \vdots & \vdots & \vdots & \vdots & \vdots \\ 0 & 0 & 0 & \cdots & -\mathbf{I} & \mathbf{I} \end{bmatrix}, \quad (23)$$

$$\tilde{\mathbf{G}} = \begin{bmatrix} \frac{\Delta z}{2} \mathbf{G}_1 & 0 & \cdots & 0 & 0 \\ 0 & \frac{\Delta z}{2} \mathbf{G}_2 & \cdots & 0 & 0 \\ \vdots & \vdots & \ddots & \vdots & \vdots \\ 0 & 0 & \cdots & \frac{\Delta z}{2} \mathbf{G}_M & 0 \\ 0 & 0 & \cdots & 0 & \frac{\Delta z}{2} \mathbf{G}_{M+1} + \frac{1}{R_L} \end{bmatrix}, \quad (24)$$

$$\tilde{\mathbf{C}} = \begin{bmatrix} \frac{\Delta z}{2} \mathbf{C}_1 & 0 & \cdots & 0 & 0 \\ 0 & \frac{\Delta z}{2} \mathbf{C}_2 & \cdots & 0 & 0 \\ \vdots & \vdots & \ddots & \vdots & \vdots \\ 0 & 0 & \cdots & \frac{\Delta z}{2} \mathbf{C}_M & 0 \\ 0 & 0 & \cdots & 0 & \frac{\Delta z}{2} \mathbf{C}_{M+1} \end{bmatrix}, \quad (25)$$

$$\tilde{\mathbf{L}} = \begin{bmatrix} \Delta z \mathbf{L}_1 & 0 & \cdots & 0 & 0 \\ 0 & \Delta z \mathbf{L}_2 & \cdots & 0 & 0 \\ \vdots & \vdots & \ddots & \vdots & \vdots \\ 0 & 0 & \cdots & \Delta z \mathbf{L}_M & 0 \\ 0 & 0 & \cdots & 0 & \Delta z \mathbf{L}_{M+1} \end{bmatrix}, \quad (26)$$

$$\tilde{\mathbf{R}} = \begin{bmatrix} \Delta z \mathbf{R}_1 & 0 & \cdots & 0 & 0 \\ 0 & \Delta z \mathbf{R}_2 & \cdots & 0 & 0 \\ \vdots & \vdots & \ddots & \vdots & \vdots \\ 0 & 0 & \cdots & \Delta z \mathbf{R}_M & 0 \\ 0 & 0 & \cdots & 0 & \Delta z \mathbf{R}_{M+1} \end{bmatrix}, \quad (27)$$

$$\mathbf{V} = [\mathbf{V}_1 \ \mathbf{V}_2 \ \cdots \ \mathbf{V}_{M+1}]^T, \quad (28)$$

$$\mathbf{I} = [\mathbf{I}_1 \ \mathbf{I}_2 \ \cdots \ \mathbf{I}_{M+1}]^T. \quad (29)$$

Notably, the number of difference segments must be a positive integer multiple of the number of cascade segments when (20) and (21) are used to solve the crosstalk of handmade cable bundles.

IV. VERIFICATION AND ANALYSIS

Taking the seven-core handmade cable bundles as an example, the radius of each wire is 0.4 mm, the insulation thickness is 0.6 mm, and the insulation material is polyvinyl chloride (PVC) with relative permittivity of 2.7, the length is 3 m, and the termination impedance of both ends is 50 Ω . Cable bundle is close to the copper current return plane.

A. Deviation rate of inductance and capacitance parameter matrix

The relative deviation rate curves of the \mathbf{L} and \mathbf{C} parameter matrix with different rotation degrees are shown in Figures 6 and 7, respectively. The reference cross section is selected as the initial cross section, that is, the degree of rotation is 0° . The relative deviation rate is obtained by the p.u.l. parameter ratio of the cross section, which is after rotating 5° , 10° , 20° , and 40° clockwise relatives to the reference plane, and the reference

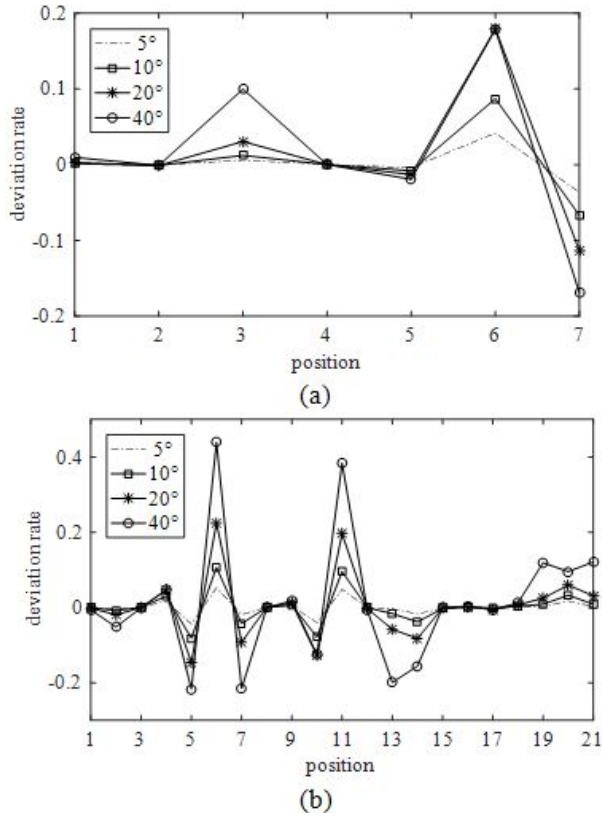


Fig. 7. Capacitance parameter deviation rate: (a) self-capacitance, (b) mutual capacitance.

cross section. Specifically,

$$\text{deviation rate} = \frac{x_{rot} - x_{ref}}{x_{ref}} \times 100\%, \quad (30)$$

where x_{ref} and x_{rot} represent the element values of the p.u.l. parameter matrix of the reference cross section and the cross section after rotation change, respectively.

The deviation rates of self-capacitance, mutual capacitance, self-inductance, and mutual inductance increase with the increase of rotation degree in Figures 7 and 8. The maximum deviation rates in different cases are given in Table 1. The maximum deviation rates of the four parameters for the 5° are small, which are 3.8%, 3.1%, 2.6%, and 5.6% respectively. Therefore, the rota-

Table 1: Maximum deviation rate of parameter matrix under different degrees of rotation

Angle	Capacitance		Inductance	
	Self	Mutual	Self	Mutual
5°	3.8%	3.1%	2.6%	5.6%
10°	8.4%	10.1%	7.5%	12.8%
20°	17.9%	22.9%	14.9%	26.2%
40°	17.9%	43.6%	29.8%	50.9%

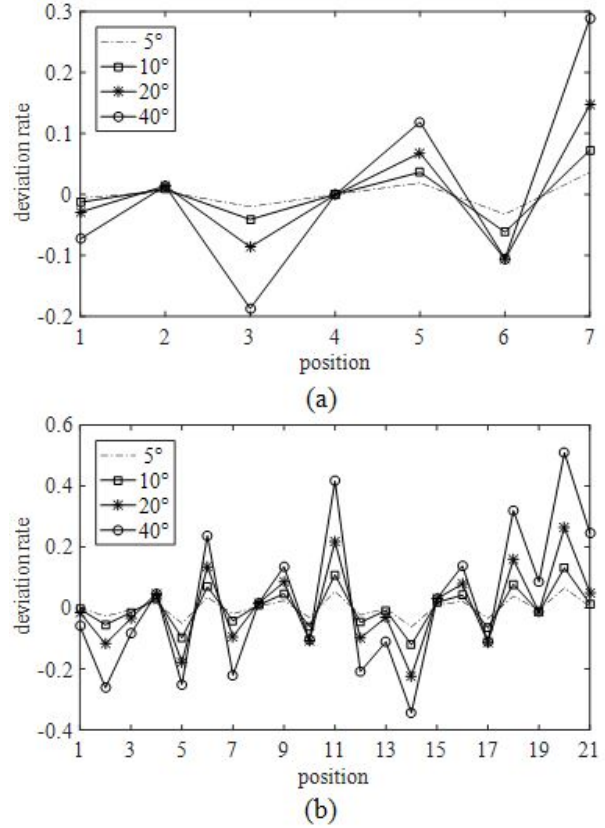


Fig. 8. Inductance parameter deviation rate: (a) self-inductance, (b) mutual inductance.

tion degree interval of the parameter matrix library for solving crosstalk is selected as 5° .

B. Crosstalk

The solution result of the near-end crosstalk of the handmade cable bundles is shown in Figure 9 when the twisting degree $\beta = 2$. The thick black dashed line and

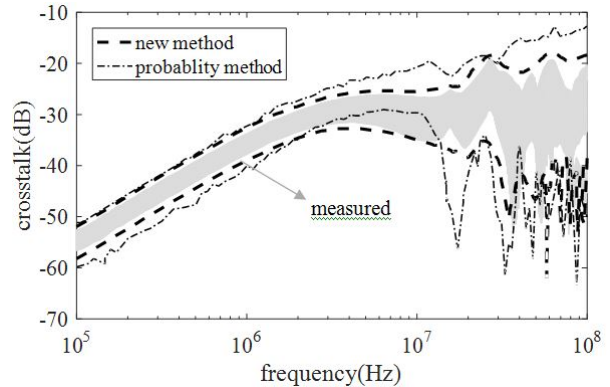


Fig. 9. Near-end crosstalk of the seven-core handmade cable bundles.

Table 2: Absolute values of upper and lower envelope error compared with the measured values

Frequency (Hz)	New Method		Probability Method	
	Upper	Lower	Upper	Lower
10^5	0.73dB	1.10dB	0.73dB	3.13dB
10^6	1.01dB	1.10dB	1.62dB	2.76dB
10^7	1.09dB	0.36dB	5.84dB	5.17dB
10^8	1.73dB	4.93dB	7.49dB	15.02dB

thin black ant line are the upper and lower envelope of the solution result of the proposed method and probability method [20], respectively. The upper envelope is the worst-case crosstalk. The gray area is the range of experimental values [20].

The absolute values of the upper and lower envelope error are shown in Table 2. Compared with the probability method, the proposed method has better agreement with the experimental results, especially at high frequency. Taking 10 MHz as an example, the absolute values of the upper and lower envelope error of the new method and the probability method are 1.09 dB, 0.36 dB, 5.84 dB, and 5.17 dB respectively. The proposed method has good accuracy in the frequency band of 100 kHz–20 MHz. However, the accuracy of the proposed method is reduced in the frequency band of 20 MHz–100 MHz, which is mainly due to the high frequency characteristics of experimental equipment. The worst-case crosstalk predicted by the proposed method can accurately reflect the actual crosstalk of the handmade cable bundles.

V. CONCLUSION

This paper proposes a novel prediction method of crosstalk for handmade cable bundles. The proposed method studies the cable bundles model from the outer- and inner-layer topology of the cross section. By considering the rotation angle of the cross section to the reference plane, the cascade harness model can be closer to the actual handmade cable bundles. The crosstalk of handmade cable bundles can be predicted by combining the unconditionally stable FDTD method. The rotation of the cross section relative to the reference plane cannot be ignored, which is verified by the deviation rate of the p.u.l. parameter matrix under different rotation angles. The technique is verified by an example of seven-core handmade cable bundles. Compared with the experimental results, the proposed method has higher precision than the probability method.

REFERENCES

- [1] S. Chabane, P. Besnier, and M. Klingler, “An embedded double reference transmission line theory applied to cable harnesses,” *IEEE Trans. Electromagn. Compat.*, vol. 60, no. 4, pp. 981-990, Aug. 2018.
- [2] S. Chabane, P. Besnier, and M. Klingler, “A modified enhanced transmission line theory applied to multiconductor transmission lines,” *IEEE Trans. Electromagn. Compat.*, vol. 59, no. 2, pp. 518-528, Apr. 2017.
- [3] C. R. Paul, “Sensitivity of crosstalk to variations in cable bundles,” *Proc. 1987 IEEE Int. Symp. EMC*, pp. 617-622, 1987.
- [4] P. Besnier and P. Degauque, “Electromagnetic topology: investigations of non-uniform transmission line networks,” *IEEE Trans. Electromagn. Compat.*, vol. 37, no. 2, pp. 227-233, May 1995.
- [5] A. Ciccolella and F. G. Canavero, “Stochastic prediction of wire coupling interference,” *Proc. 1995 IEEE Int. Symp. EMC*, pp. 51-56, 1995.
- [6] S. Salio, F. Canavero, D. Lecointe, and W. Tabbara, “Crosstalk prediction on wire bundles by Kriging approach,” *IEEE Int. Symp. Electromagn. Compat.*, pp. 197-202, 2000.
- [7] S. Sun, G. Liu, J. Drewniak, and D. Pommerenke, “Hand-assembled cable bundle modeling for crosstalk and common-mode radiation prediction,” *IEEE Trans. Electromagn. Compat.*, vol. 49, no. 3, pp. 708-718, Aug. 2007.
- [8] M. Wu, D. Beetner, T. Hubing, H. Ke, and S. Sun, “Estimation of the statistical variation of crosstalk in wiring harnesses,” *2008 IEEE Int. Symp. Electromagn. Compat.*, 2008, pp. 1-7.
- [9] M. Wu, D. G. Beetner, T. H. Hubing, H. Ke, and S. Sun, “Statistical Prediction of “Reasonable Worst-Case” Crosstalk in Cable Bundles,” *IEEE Trans. Electromagn. Compat.*, vol. 51, no. 3, pp. 842-851, Aug. 2009.
- [10] G. Spadacini, F. Grassi, and S. A. Pignari, “Field-to-wire coupling model for the common mode in random bundles of twisted-wire pairs,” *IEEE Trans. Electromagn. Compat.*, vol. 57, no. 5, pp. 1246-1254, Oct. 2015.
- [11] S. A. Pignari, G. Spadacini, and F. Grassi, “Modeling field-to-wire coupling in random bundles of wires,” *IEEE Electromagn. Compat. Mag.*, vol. 6, no. 3, pp. 85-90, Third Quarter 2017.
- [12] V. Ramesh Kumar, A. Alam, B. K. Kaushik, and A. Patnaik, “An unconditionally stable FDTD model for crosstalk analysis of VLSI interconnects,” *IEEE Trans. Compon., Packag. Manuf. Technol.*, vol. 5, no. 12, pp. 1810-1817, Dec. 2015.
- [13] C. Huang, Y. Zhao, W. Yan, Q. Liu, and J. Zhou, “A new method for predicting crosstalk of random cable bundle based on BAS-BP neural network algorithm,” *IEEE Access*, vol. 8, pp. 20224-20232, Jan. 2020.
- [14] Z. Pei, X. Li, Y. Li, and J. Mao, “Transient coanalysis of multicoupled passive transmission lines and

- Josephson junctions based on FDTD," *IEEE Trans. Appl. Supercond.*, vol. 30, no. 1, pp. 1-7, Jan. 2020.
- [15] F. Zheng and Z. Chen, "Numerical dispersion analysis of the unconditionally stable 3-D ADI-FDTD method," *IEEE Trans. Microw. Theory Tech.*, vol. 49, no. 5, pp. 1006-1009, May 2001.
- [16] F. Zheng, Z. Chen, and J. Zhang, "A finite-difference time-domain method without the Courant stability conditions," *IEEE Microw. Guided Wave Lett.*, vol. 9, no. 11, pp. 411-443, Nov. 1999.
- [17] M. Tang and J. Mao, "A precise time-step integration method for transient analysis of lossy nonuniform transmission lines," *IEEE Trans. Electromagn. Compat.*, vol. 50, no. 1, pp. 166-174, Feb. 2008.
- [18] K. Afrooz and A. Abdipour, "Efficient method for time-domain analysis of lossy nonuniform multiconductor transmission line driven by a modulated signal using FDTD technique," *IEEE Trans. Electromagn. Compat.*, vol. 54, no. 2, pp. 482-494, Apr. 2012.
- [19] C. R. Paul, *Analysis of Multiconductor Transmission Lines*, New York, USA: Wiley, 1994.
- [20] Z. Zhang, S. Wang, and L. Zhao, "Prediction of crosstalk probability distribution in cable bundles," *Transactions of China Electrotechnical Society*, vol. 32, no. 7, pp. 203-214, Apr. 2017.



Jinghua Guo graduated from Northeast Agricultural University in July 1989, majoring in mechanization. He is currently an associate professor in Wuxi Vocational College of Science and Technology. Mr. Guo's current research directions are automotive electricians & electronics, automotive electromagnetic compatibility, automotive electronic control technology, automotive network technology, and new energy vehicles.



Yuanyuan Liu was born in Shandong, China, in 1983. She received her B.S. degree in mechanical manufacturing and automation from Shandong University of Technology, Zibo, China, in 2004, M.S. degree in mechanical manufacturing and automation from Nanjing University of Aeronautics and Astronautics, Nanjing, China, in 2007. Ms. Liu is currently pursuing Ph.D. in control theory and control engineering in Jiangnan University, Wuxi, China. She is also an associate professor in Wuxi Vocational College of Science and Technology. Her current research interests include electric control technology and wireless power transfer technology of electric vehicles.